Journal of Applied Polymer Science

Polyaniline/Ag Nanocomposite Synthesized by Using Aniline as Dispersant and Stabilizer of Nanosilver Sol

Zhihua Li,[1,2] Yanbo Li,[1,2] Jianti Lu,[1,2] Feng Zheng,[1,2] Jozua Laven,[3] Adolphe Foyet[3]

[1]Key Laboratory of Nonferrous Metal Materials Science and Engineering of Ministry of Education, Central South University, Changsha 410083, People's Republic of China

[2]School of Materials Science and Engineering, Central South University, Changsha 410083, People's Republic of China

[3]Laboratory of Materials Science and Interfaces, Faculty of Chemical Engineering and Chemistry, Eindhoven University of Technology, 5600 MB, Eindhoven, The Netherland

Correspondence to: Zhihua Li (E-mail: ligfz@mail.csu.edu.cn)

ABSTRACT: Polyaniline/silver (PANI/Ag) nanocomposite was successfully prepared by in-situ polymerization from nanosilver sol using aniline (An) as both dispersant and stabilizer and characterized by FT-IR, XRD SEM, TEM and electrochemical methods, respectively. The results showed that core-shelled composite particles of less than 100 nm were synthesized with PANI as shell formed around a core of silver nanoparticles at higher aniline levels. Compared to pure PANI, PANI/Ag nanocomposites have higher electrical conductivity (65.98 S/cm) and current response and capacitance as well. Potentio dynamic polarization showed the anodic shifting of zero current potential and a lower exchange current density for the PANI/Ag composite. Compared with PANI, the PANI/Ag nanocomposite is a promising candidate for coatings with improved anti-corrosion performance. © 2012 Wiley Periodicals, Inc. J. Appl. Polym. Sci. 128: 3933–3938, 2013

KEYWORDS: composites; nanoparticles; nanowires; nanocrystals; surfactants; synthesis and processing; conducting polymers

Received 26 July 2012; accepted 20 September 2012; published online 16 October 2012
DOI: 10.1002/app.38618

INTRODUCTION

When compared to other conductive polymers such as polypyrrole (PPy), polythiophene (PTH), poly-*p*-phenylene (PPP), and poly-*p*-phenylene vinylene (PPV), polyaniline (PANI) is easy to prepare and has good environmental stability. PANI has wide applications in electrode material, energy storage, electromagnetic shielding, biosensors, and anticorrosion materials.[1–6] In the domain of functional materials, PANI is also attractive as base matrix for many metal-organic composites. Several metal-PANI composites such as PANI/Pd,[7] PANI/Pt,[8] PANI/Au,[9] PANI/Co,[10] PANI/Cu,[11] and PANI/Ag[12] have been prepared. These composites display not only higher modulus, heat resistance, surface hardness, and conductivity but can also use for corrosion protection, electrocatalysis, biosensor, and hydrogen storage. Recent studies showed that PANI/Pd and PANI/Pt exhibit a very good catalytic properties and electrochemical activity.[13,14] Because of easy preparation, low cost, and high electrical conductivity, PANI/Ag nanocomposite has wide and attractive applications in many fields, such as antibacterials, conductive coating, adhesives, electrochemical sensors, etc. PANI/Ag nanocomposite becomes one of the most important metal-polymers with multifunction.

PANI/Ag nanocomposite is commonly synthesized in the presence of metallic particles, by either oxidation of aniline with metallic compounds or using PANI as a reductant of metal salt or acid.[15] All these methods require at least one surfactant in order to reduce the size of metallic particles.[16–18] It is difficult completely to remove surfactant from final product. The remaining surfactant serves as impurity, which may have negative effects on electrical, optical, and mechanical properties of the materials. Although advanced techniques such as microwave, γ ray and ultrasonic wave being used to reduce the content of residual surfactant,[19–22] the size and morphology of composite particles are still difficult to control. On the other hand, cost and experimental constraints of aforementioned equipments may limit their applications. Therefore, it is interesting to find a simple and efficient method to synthesis PANI/Ag nanocomposite with less impurity. It is therefore the objective of our work to find out such a method.

In our work, a novel and efficient method was put forward for the preparation of nanosilver sol and PANI/Ag nanocomposite. Sodium hypophosphite was chosen as an efficient reducing agent and aniline was used both as dispersant and stabilizer in the formation of nanosilver sol. PANI/Ag nanocomposite was successfully prepared by *in situ* polymerization of the aniline

Applied Polymer SCIENCE

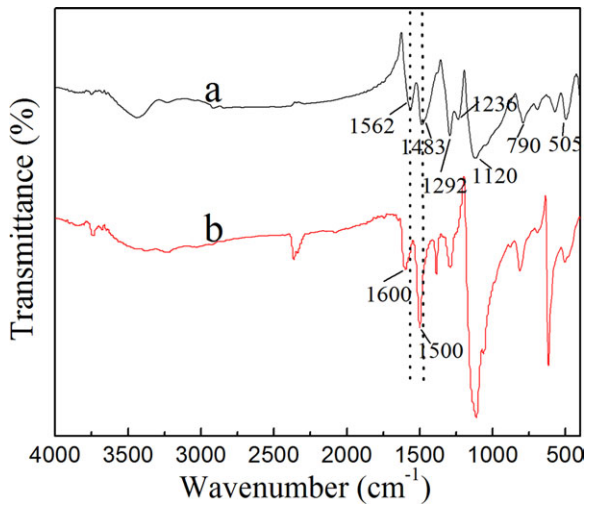

Figure 1. FTIR spectra of (a) PANI and (b) PANI/Ag nanocomposite. [Color figure can be viewed in the online issue, which is available at wileyonlinelibrary.com.]

around silver nanoparticles. This method has several distinctive features among which simplicity, high efficiency, and yield, less impurity as consequence of the absence of surfactant. The formation of composite particles with core-shell structure and low impurity may have significant impact on the electrical properties of this material. The microstructure and the electrical properties of this nanocomposite material were determined by using physical and electrochemical techniques in details.

EXPERIMENTAL

Synthesis

All reagents (aniline, silver nitrate, sodium hypophosphite, and ammonium persulfate) were analytical grade and commercially available from local chemical shops.

Nanosilver sol was prepared in three steps. A certain amount of sodium hypophosphite was first dissolved into distilled water (solution A) and stirred uniformly for 10 min by using ultrasonic wave. A second solution (solution B) containing a certain ratio of aniline and nitric acid (1 mol/L) was prepared. In the second step, solutions A and B were mixed together and stirred uniformly. Nanosilver sol was obtained by adding drops of silver nitrate solution gradually into reactor under stirring condition. The mixture was maintained at 40°C for 90 min to complete the reaction.

The nanosilver sol was cooled down to room temperature. An aqueous solution containing ammonium persulfate and nitric acid (1 mol/L) was dropped into the sol and stirred for 4 h at room temperature. The final solution was centrifuged and the precipitate was washed three times, with ethanol, acetone, and distilled water, respectively. The product was dried in an oven at 60°C for 24 h to get PANI/Ag nanocomposite.

Characterization

Fourier transform infrared spectroscopy (FTIR) analysis was performed with a NICOLET 6700 spectrophotometer in the wave number ranging from 4000 to 400 cm^{-1}. Samples were prepared into KBr pellets. X-ray diffraction (XRD) spectrum of the sample was recorded with Cu Kα radiation ($\lambda = 1.54$ Å) in the diffractometer (model D/Max 2550). Microstructure of composite was determined by transmission electron microscopy (TEM, Model Tecnai $G^2$20ST) and scanning electron microscopy (SEM, Model Sirion 200). Electrical conductivity of compressed composite pellets with diameter of 14 mm (prepared under 20 MPa) was measured at room temperature by four-probe method. Electrochemical behavior of the composites were studied in 0.5*M*/L H_2SO_4 by using Pt as counter electrode, saturated calomel electrode as reference electrode and PANI/Ag as working electrode. Cyclic voltammograms (CV) were recorded at 50 mV/s by using a Zahner (IM6ex, Germany) electrochemical station. Impedance spectrum (EIS) of the sample was also recorded in H_2SO_4 solution under open circuit potential for frequencies ranging from 100 kHz to 5 mHz using 5 mV ac amplitude of sinusoidal voltage.

RESULTS AND DISCUSSION

Structure Characterization

FTIR is a powerful tool to determine the vibration and stretching bands of functional groups in organic molecules. Figure 1 displayed the FTIR spectrum of both PANI and PANI/Ag composite. The main bands observed for PANI (Figure 1a) at 1562 and 1483 cm^{-1} were attributed to quinonoid (Q) and benzenoid (B) ring-stretching vibrations.[23,24] The absorption band at about 1236 and 1292 cm^{-1}corresponded to C—N stretching of structure B and Q.[25] Peak at 1120 cm^{-1} was considered as bending vibration of C—H in benzene ring. Absorption bands at 790 and 505 cm^{-1}were attributed to plane bending vibration of C—N for 1,4 substitute position of benzene ring and bending vibration of benzene ring, respectively.[26] Spectrum of PANI/Ag (Figure 1b) was comparable to that of PANI although some peaks were not fully identical. Vibrations of Q and B were shifted from 1562 and 1483 cm^{-1} to 1600 and 1500 cm^{-1}, respectively. This phenomenon is explained as that: A large number of electrons around silver atoms tend to conjugate Q and B structure due to electrostatic interaction between electrons and aniline cation. Consequently, a large scale of electron cloud is formed between silver and aniline and leads to shift of infrared absorption.

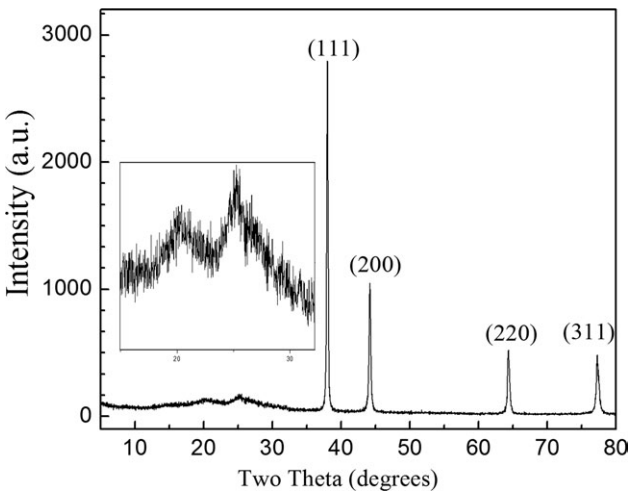

Figure 2. XRD spectra of PANI/Ag nanocomposite.

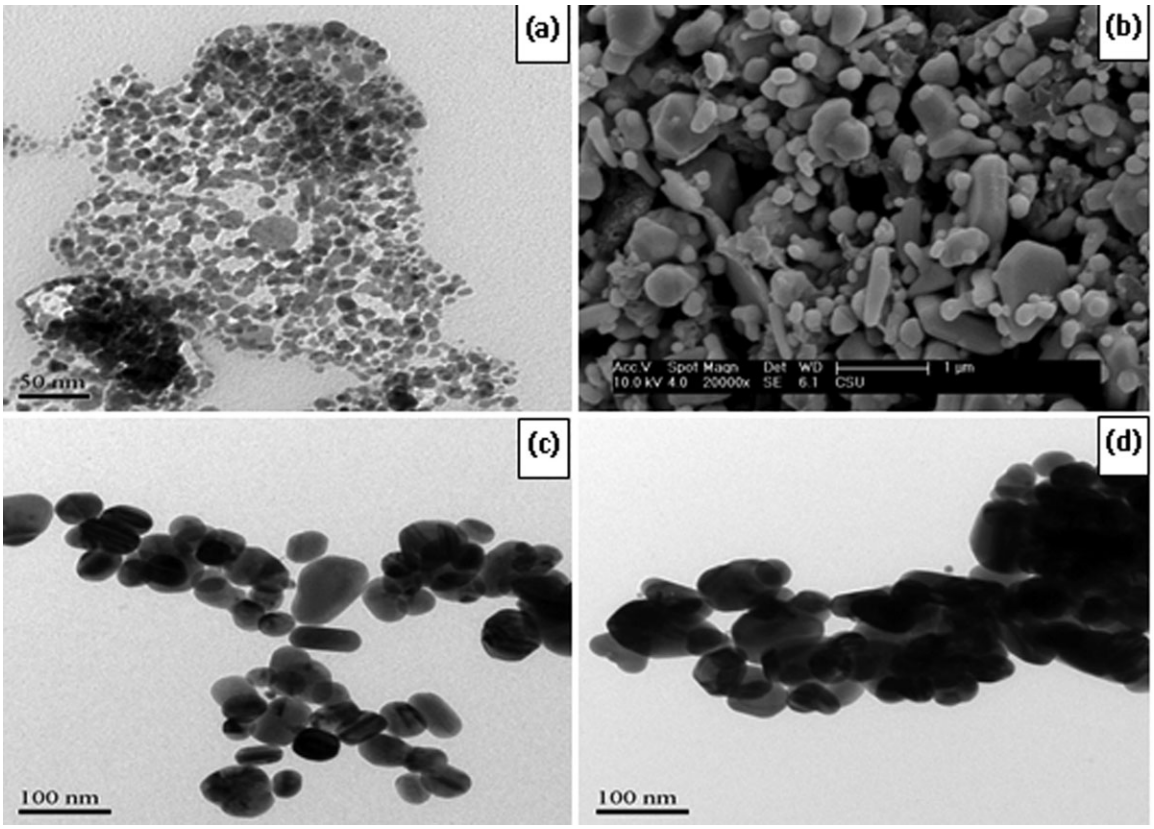

Figure 3. TEM and SEM images of silver nanoparticles and PANI/Ag nanocomposites: (a) TEM image of silver nanoparticles and (b) SEM image of PANI/Ag nanocomposite; (c, d) TEM images of PANI/Ag nanocomposites. The ratio R is 1 : 3 for (b, c) and 1 : 1 for (d).

XRD pattern of the product was shown in Figure 2. The diffraction peaks at $2\theta = 37.9°$, 44.1°, 62.3°, and 77.3° can be assigned to Bragg's reflections from (111), (200), (220), and (311) planes of silver. This result is in agreement with standard spectrum (JCPDS NO.4-0783) of crystalline silver. This confirms the presence of metallic silver in nanocomposite. The relation between grain size and peak width of XRD peaks was given by Scherrer equation [eq. (1)].[27]

$$d = K\lambda/(B\cos\theta) \quad (1)$$

where λ is the wavelength ($\lambda = 1.54056$ Å for Cu Kα), θ is the diffraction angle, B is the width at half height of the peak around θ, K is the correction factor ($K = 0.9$). The size of every crystal face, as calculated according to benchmark of standard silver peaks, was 56, 37, 41, and 43 nm, respectively.

There are two small peaks at low diffraction angle ($2\theta = 20°$ and 25°), which can be assigned to PANI.[28,29] The sharpness (width) of these peaks represented the degree of orientation of PANI chains in that particular crystal plane, and the intensity (peak height) stands for population of crystallites in that plane. In our case, the peaks were not sharp due to the poor orientation of PANI chains. The low degree of crystallization of PANI is probably due to its combination with silver nanoparticles.

Morphology of Nanocomposite

Morphology of nanocomposite was determined by SEM and TEM, respectively. Figure 3 displayed the morphology of silver nanoparticles and PANI/Ag nanocomposite as synthesized at different aniline-to-$AgNO_3$ ratios (R).

As can be seen from image (a), silver nanoparticles, the intermediates, take on spherical particles with the diameter of less than 50 nm. Because of the conjugating effect of electron cloud, dispersion between silver particles is also improved. Images (b) and (c) display the morphology of PANI/Ag nanocomposite prepared when R is 1 : 3. By comparison with image (a), the

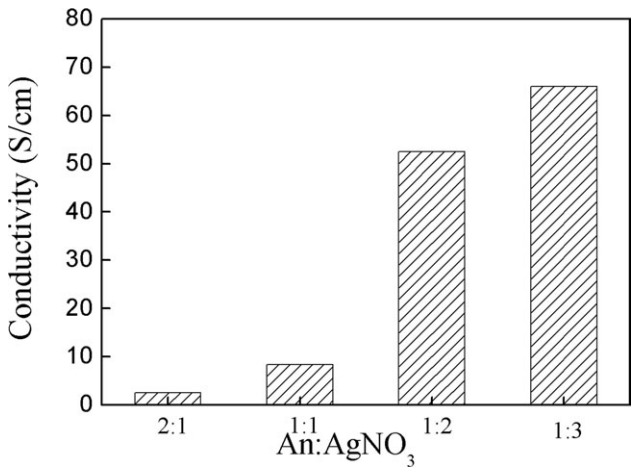

Figure 4. Conductivity of PANI/Ag nanocomposite as function of the An : $AgNO_3$ ratio.

Applied Polymer SCIENCE

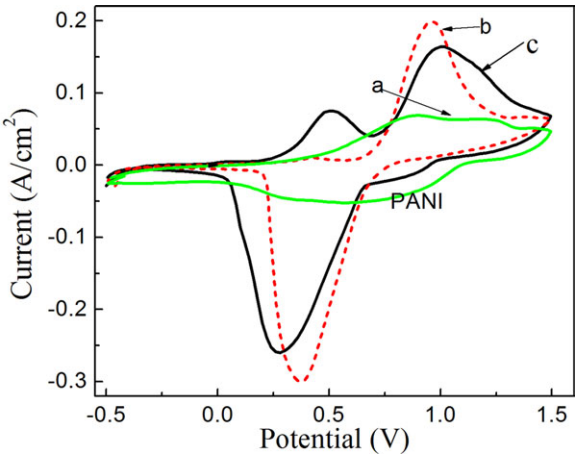

Figure 5. CV of (a) PANI and nanocomposite with An : $AgNO_3$ ratio (b) 1 : 3 and (c) 2 : 1 in 0.5*M*/L H_2SO_4. All potentials were giving with respect to saturated calomel electrode, scan rate 50 mV/s. [Color figure can be viewed in the online issue, which is available at wileyonlinelibrary.com.]

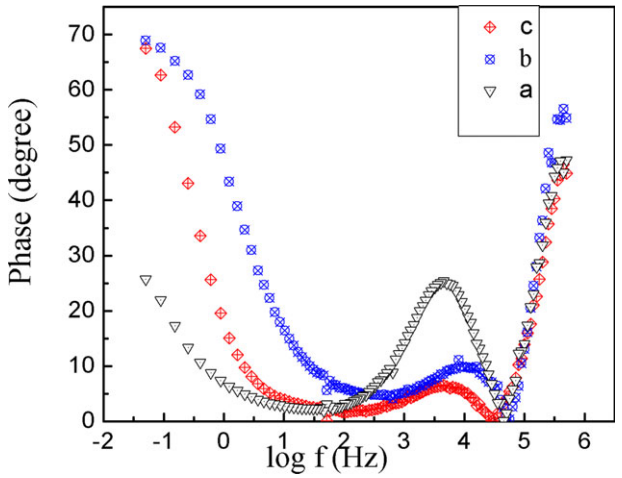

Figure 7. Phase angle of (a) PANI, PANI/Ag with *R* ratio (b) 1 : 3 and (c) 2 : 1 in 0.5*M*/L H_2SO_4. [Color figure can be viewed in the online issue, which is available at wileyonlinelibrary.com.]

dark spots in image (c) should correspond to silver nanoparticles while the light ones are PANI. Most of silver nanoparticles are not coated fully by PANI but partly when *R* is low. Consequently, there are dark lines or small spots appearing on the surface of PANI particles. This reveals that at low amount of aniline, it is difficult to form perfect PANI layers on the surface of silver nanoparticles. On the contrary, PANI appears easily on the form of irregular block, which is showed in image (b). With increasing of the use of aniline, to form PANI layers on the surface of silver nanoparticles is easier and core-shelled structure is also gradually formed. Just as displayed as image (d), a large amount of aniline contributes to the formation of PANI layers but also results in bad dispersion between composite particles.

From above analysis, it can be seen that the amount of aniline plays a significant role in the dispersion and morphology of composite nanoparticles. Aniline molecular is helpful for the dispersion between silver nanoparticles because of its adsorption ability on the surface of silver nanoparticles. Too small dosage can not form ideal core-shelled structure but too large amount would result in bad dispersion between composite particles. Therefore, the value of *R* is considered as an important factor to affect the structure and morphology of nanocomposite.

Electrical Conductivity

Electrical conductivity of PANI/Ag nanocomposite was tested by four-probe method. Figure 4 shows the conductivity of composites prepared at different amounts of aniline. It can be observed that electrical conductivity of composite increase when the amount of aniline in reacting mixture decreases. Conductivity value of 65.98 S/cm was achieved when *R* was 1 : 3. The addition of aniline has reducing effect on conductivity of nanocomposite. This tendency is normal because silver particles have higher conductivity and the addition of any polymer matrix, which is less conductive, can only reduce conductivity of

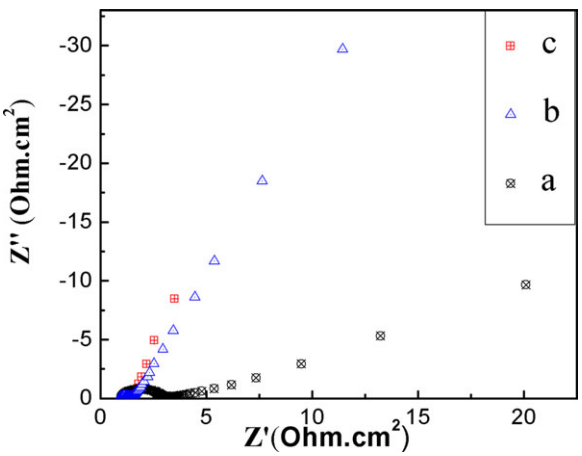

Figure 6. Nyquist representation of (a) PANI, PANI/Ag with *R* ratio (b) 1 : 3 and (c) 2 : 1 in 0.5*M*/L H_2SO_4. [Color figure can be viewed in the online issue, which is available at wileyonlinelibrary.com.]

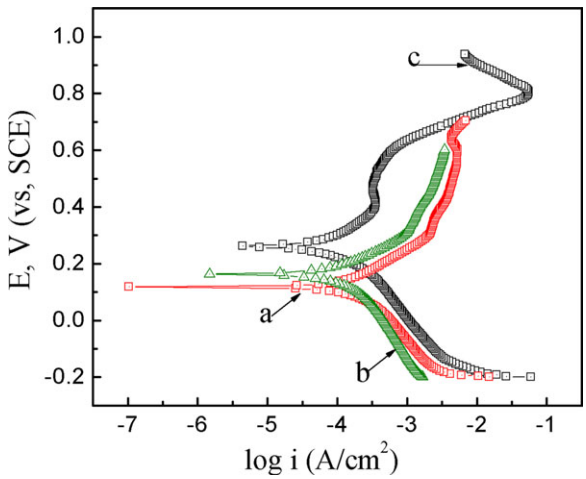

Figure 8. Polarization curve of (a) PANI and PANI/Ag nanocomposite with (b) *R* = 1 : 3 and (c) 2 : 1 in 0.5*M*/L H_2SO_4. [Color figure can be viewed in the online issue, which is available at wileyonlinelibrary.com.]

Table I. Density of Corrosion Current of Different Samples

Samples	a	b	c
Density of corrosion current for different samples in 0.5M/L H_2SO_4 ($\mu A/cm^{-2}$)	106.0	91.8	67.9

composite. Conductivity tendency is also in agreement with the morphology of nanocomposite clusters as shown by SEM and TEM. At low amount of aniline, silver nanoparticles came together easily, which was suitable for electron conduction. On the contrary, large amount of aniline in reacting mixture contributes to the isolation of silver nanoparticles and leads to perfect shelled with low conductivity.

Electrochemical Performance

To determine electrochemical performance of PANI/Ag nanocomposite, working electrodes (made of PANI or PANI/Ag, acetylene black and polytetrafluoroethylene(PTEF) at composition ratio of 8 : 1 : 1) were investigated in 0.5 M/L H_2SO_4 by the CV method. Results are showed in Figure 5.

Curve of pure PANI (Figure 5a) has a small area as compared to PANI/Ag curves (b) and (c). This reveals that the capacitance of pure PANI is smaller than that of the nanocomposite. Peak at 0.77 V can be attributed to oxidation process (N = Q = N group) of PANI. Peak at 1.0 V is assigned to the oxidation of Ag. This last peak became smaller and its oxidation potential shifts slightly to a positive value as the amount of aniline increasing. Silver nanoparticles are surrounded by PANI layers and large amounts of aniline leads to greater interfacial action between Ag and PANI. Electronic transfer between silver nanoparticles is more restricted. As a consequence, the oxidation peak current of silver decreased and the capacitance of the system increased. Besides, response current of composite is higher than the one of PANI indicating that the electrochemical activity of the PANI/Ag electrode is improved. This result is in agreement with the conductivity measurement. PANI is less conductive and the addition of conductive particles will increase conductivity.

Electrochemical impedance spectra of electrodes modified with PANI and PANI/Ag nanocomposite were recorded in 0.5*M* H_2SO_4 solution. Nyquist representation (Figure 6) and phase angle (Figure 7) of modified electrodes are displayed.

For all samples, Nyquist plots show a semi-circle at high frequency and a straight line at low frequency. Such Nyquist shape is the character of most conductive polymers. The intercept of the high frequency semi-circle with real axis represents the charge transfer resistance of modified electrode. Diameter of this high frequency semi-circle is smaller in nanocomposite as compared to PANI. This suggests that charge transfer resistance (R_c) of PANI modified electrode is higher. Impedance results are in agreement with the conductivity measurement; all show that resistance of PANI decreases when silver nanoparticles are incorporated. It is also important to notice that the slope of low frequency line is higher in nanocomposite as compared to pure PANI. At the same time, the phase angle of nanocomposites tends to 90° at low frequency. All reveal that the capacitance of the composite was greater than that of pure PANI. As a conclusion, electrical behavior of PANI has been changed from resistive to capacitive systems by incorporation of sufficient silver nanoparticles. Such capacitive nanocomposite shows promising application in corrosion protection of metallic parts for which complete electrical isolation is not required.

Figure 8 shows the polarization curves of PANI and PANI/Ag modified electrodes in 0.5*M*/L H_2SO_4. Corrosion potential shifts in the anodic direction when silver nanoparticles are present in PANI. This indicates that PANI/Ag nanocomposite provides better protection as compared to pure PANI. This protective ability is more pronounced for composite synthesized from a mixture containing high amount of aniline. Corrosion current density was calculated from the anodic branch of polarization curves and results were summarized in Table I. Corrosion current density is higher in the case of aniline but decreases significantly in the case of PANI/Ag nanocomposite.

A very low corrosion current was achieved with a reaction mixture containing high amount of aniline (curve c). In this case, the anodic branch of polarization curve shows a passive region from 0.4 to 0.55 V in polarization plot followed by a breakdown

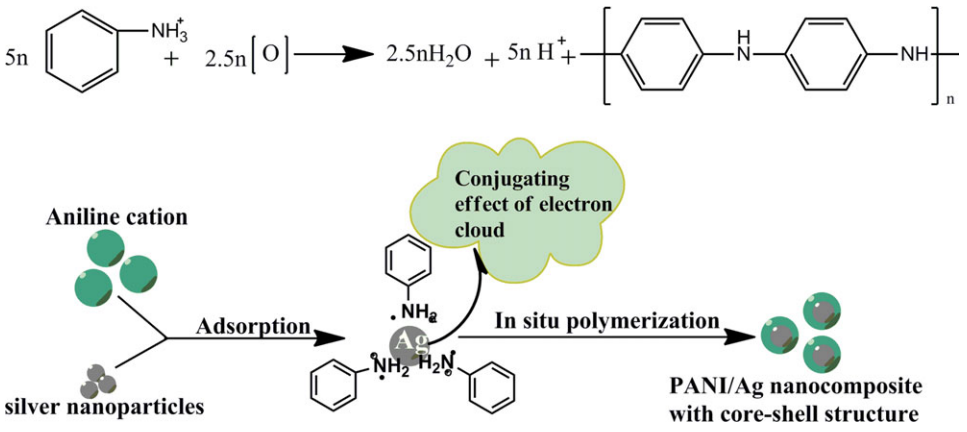

Figure 9. Formation mechanism of PANI/Ag nanocomposite. [Color figure can be viewed in the online issue, which is available at wileyonlinelibrary.com.]

potential at around 0.6 V in plot. The presence of a passive region in curve confirms capacitive tendency or barrier properties of this sample. Similar results are obtained from impedance measurements.

Formation Mechanism of PANI/Ag Nanocomposite

Generally, a large number of electrons around silver atoms easily conjugate with Q and B structure and finally form a large scale of electron cloud (shown as Figure 9). So after the reduction process of Ag^+ to Ag, aniline molecular naturally adsorbs on the surface of silver nanoparticles. Under stirring, many aniline monomers form a stable shelled around silver nanoparticles and prevent their agglomeration. As a consequence, the sol remained stable without additional surfactant. The addition of initiator induces the oxidation of adsorbed aniline monomers (to $C_6H_5NH_3^+$) and starts polymerization process. When concentration of aniline is high, PANI chains will grow easily around silver nanoparticles and form a core-shelled structure according to the mechanism displayed in Figure 9. It is also showed that the size of the composite clusters can be controlled by adjusting concentration of aniline in the starting mixture.

CONCLUSION

PANI/Ag nanocomposite was synthesized successfully from a nanosilver sol prepared without additional surfactant. In the preparation of nanocomposite, aniline not only played the role of dispersant and stability, but also contributed to the formation of core-shelled structure of composite. The amount of aniline has an significant effect on the morphology of nanocomposite. A small ratio did not contribute to the formation of PANI layers. When *R* increases to 2 : 1, the tendency of silver nanoparticles to agglomerate is greatly reduced and PANI coating becomes more compact leading to a pronounced core-shelled structure. Even so, larger value of *R* also results in bad dispersion between composite particles. Electrical conductivity of nanocomposite increases with the concentration of silver nanoparticles increasing while capacitance is higher for samples containing more aniline in the starting mixture. Electrochemical properties of nanocomposite materials are improved as compared to pure PANI. This kind of nanocomposite shows promising application in corrosion protection of metallic parts for which complete electrical isolation is not required.

REFERENCES

1. Gupta, K.; Jana, P. C.; Meikap, A. K. *Synth. Met.* **2010**, *160*, 1566.
2. Afzal, A. B.; Akhtar, M. *J. Chin. Phys. B.* **2011**, *5*, 058102–1.
3. Sathiyanarayanan, S.; Muthkrishnan, S.; Venkatachari, G. *Electrochim. Acta* **2006**, *51*, 6313.
4. Souza, S. D. *Surf. Coat Technol.* **2007**, *201*, 7574.
5. Tahir, Z. M.; Alocilja, E. C.; Grooms, D. L. *Biosens. Bioelectron* **2005**, *20*, 1690.
6. Yan, W.; Feng, X. M.; Li, X. H.; Zhu, J. *J. Bioelectrochemistry* **2008**, *72*, 21.
7. Daisuke, S.; Toru, A.; Toshikazu, H. *J. Inorg. Organomet. Polym.* **2009**, *19*, 79.
8. Huang, L.-M.; Liao, W.-H.; Ling, H.-C.; Wen, T.-C. *Mater. Chem. Phys.* **2009**, *116*, 474.
9. Gupta, K.; Jana, P. C.; Meikap, A. K. *Solid State Sci.* **2012**, *14*, 324.
10. Tang, L.; Wu, T.; Kan, J. Q. *Synth. Met.* **2009**, *159*, 1644.
11. Pruna, A.; Branzoi, V.; Branzoi, F. *J. Appl Electrochem* **2011**, *41*, 77.
12. Mohaseen, S.; Tamboli, M. V.; Kulkarni, R. H.; Patil, W. N.; Gade, S. C.; Navale, B.; Kale, B. *Colloids Surf B* **2012**, *92*, 35.
13. UI Islam, R.; Witcomb, M. J.; van der Lingen, E.; Scurrell, M. S.; Van Otterlo, W.; Mallick, K. *J. Organomet. Chem.* **2011**, *696*, 2206.
14. Saraswat, A.; Sharma, L. K.; Srivastava, M. K.; Siddiqui, I. R.; Singh, R. K. P. *J. Appl. Polym. Sci.* **2012**, *3*, 1479.
15. Natalia, V. B.; Jaroslav, S.; Miroslava, T.; Irina, S.; Gordana, C. M. *Polymer* **2009**, *50*, 50.
16. Zhou, D. H.; Li, Y. H.; Wang, J. Y.; Xu, P.; Han, X. *J. Mater. Lett.* **2011**, *65*, 3601.
17. Zhou, Z.; He, D. L.; Guo, Y. N.; Cui, Z. D.; Wang, M. H.; Li, G. X.; Yang, R. H. *Thin Films* **2009**, *517*, 6767.
18. Fujii, S.; Nishimura, Y.; Aichi, A.; Matsuzawa, S.; Nakamura, Y.; Akamatsu, K.; Nawafune, H. *Synth. Met.* **2010**, *160*, 1433.
19. Zhou, H. H.; Ning, X. H.; Li, S. L.; Chen, J. H.; Kuang, Y. F. *Thin Solid Films* **2006**, *510*, 164.
20. de Barros, R. A.; de Azevedo, W. M. *Synth. Met.* **2008**, *158*, 922.
21. de Barros, R. A.; de Azevedo, W. M. *Synth. Met.*, **2010**, *160*, 1387.
22. Kim, H. J.; Park, S. H.; Park, H. *J. Radiat. Phys. Chem.* **2010**, *79*, 894.
23. Tamboli, M. S.; Kulkarni, M. V.; Patil, R. H.; Gade, W. N.; Navale, S. C.; Kale, B. B. *Colloids Surf B* **2012**, *92*, 39.
24. Janosevic, A.; Pasti, I.; Gavrilov, N.; Mentus, S.; Krstic, J.; Mitric, M.; Travas-Sejdic, J.; Ciric-Marjanovic, G. *Microporous Mesoporous Mater.* **2012**, *152*, 54.
25. El-Dib, F. I.; Sayed, W. M.; Ahmed, S. M.; Elkodary, M. *J. Appl. Polym. Sci.* **2011**, DOI 10.1002/app, 3203.
26. Kumar, S.; Sharma, S. K. *J. Mater. Sci.: Mater. Electron* **2012**, *23*, 1261.
27. Nguyen, V. H.; Shim, J.-J. *Synth. Met.* **2011**, *161*, 2082.
28. Angelopoulos, M.; Dipietro, R.; Zheng, W. G.; MacDiarmid, A. G. *Synth. Met.* **1997**, *84*, 38.
29. Sambhu, B.; Dipark, K. *Polym. Test.* **2008**, *27*, 853.